

Levistilide a Induces Ferroptosis by Activating the Nrf2/HO-1 Signaling Pathway in Breast Cancer Cells

Shangwen Jing^{1,*}, Yantong Lu^{1,2,*}, Jing Zhang¹, Yan Ren^{1,2}, Yousheng Mo³, Dongdong Liu³, Lining Duan⁴, Zhongyu Yuan⁵, Changjun Wang², Qi Wang¹

¹Science and Technology Innovation Center, Guangzhou University of Chinese Medicine, Guangzhou, People's Republic of China; ²Guangdong Provincial People's Hospital, Guangdong Academy of Medical Sciences, Guangdong Geriatric Institute, Guangzhou, People's Republic of China; ³The Second Affiliated Hospital of Guangzhou University of Chinese Medicine, Guangzhou, People's Republic of China; ⁴The First Affiliated Hospital of Guangzhou University of Chinese Medicine, Guangzhou, People's Republic of China; ⁵Department of Medical Oncology, Sun Yat-Sen University Cancer Center, the State Key Laboratory of Oncology in South China, Collaborative Innovation Center for Cancer Medicine, Guangzhou, 510060, People's Republic of China

*These authors contributed equally to this work

Correspondence: Changjun Wang; Qi Wang, Email gzwchj@126.com; wangqi@gzucm.edu.cn

Introduction: Breast cancer (BC) is the leading female malignancy, with one million new cases diagnosed worldwide per year. However, the current treatment options for BC patients have difficulty achieving satisfactory efficacy. Ferroptosis is a new mode of regulated cell death that plays a key role in the inhibition of tumorigenesis. Levistilide A (LA), as an active compound extracted from *Chuanxiong* Rhizoma, might prevent the development of tumors by regulating the critical cellular processes of ferroptosis.

Methods: In this study, the underlying mechanisms of LA on ferroptosis in BC were explored in vitro. The effect of LA on the viability and mitochondrial function of BC cells was determined. Moreover, the effect of LA on the expression levels of key molecules involved in ferroptosis and the nuclear factor erythroid-2-related factor 2/heme oxygenase 1 (Nrf2/HO-1) signaling pathway was evaluated.

Results: LA significantly reduced cell viability and damaged the mitochondrial structure and function of BC cells in a dose-dependent manner. Furthermore, LA treatment markedly enhanced reactive oxygen species (ROS)-induced ferroptosis by activating the Nrf2/HO-1 signaling pathway.

Conclusion: These findings suggest that LA may be a potential lead compound for breast cancer therapy by inducing ferroptosis in tumor cells.

Keywords: breast cancer, levistilide A, ferroptosis, Nrf2/HO-1 signaling pathway

Introduction

Breast cancer (BC) is the leading female malignancy, with one million new cases diagnosed worldwide per year.¹ Although extensive progress has been made in the treatment of BC over the last few decades with surgery, targeted hormone therapy, chemotherapy and radiotherapy becoming the main treatment options for BC patients, the prognosis for BC patients remains poor because the efficacy of these interventions has been seriously compromised due to the emergence of multidrug resistance and obvious side effects.^{2,3} Therefore, studies targeting effective treatment measures with minimal side effects are necessary to expand the existing therapeutic options for BC patients.

Defects in the cell death executioner mechanism are the main reason for cancer treatment resistance.⁴ Thus, the exploration of a new form of cell death is urgently needed in BC therapy. Ferroptosis is an entirely new mode of iron-dependent and reactive oxygen species (ROS)-dependent regulated cell death that was first identified in 2012.⁵ Recent studies have pointed out that tumor cells have an increased demand for iron, which makes them more vulnerable to ferroptosis.⁶ Furthermore, the higher growth rate and oxygen requirement induce tumor cells to experience more

oxidative stress, which is a vital causative pathway to induce ferroptosis.⁷ Importantly, increasing evidence has suggested that ferroptosis plays a key role in the inhibition of tumorigenesis by efficiently clearing damaged cells and maintaining microenvironment homeostasis.^{8,9} The lethal depletion of glutathione (GSH) and glutathione peroxidase 4 (GPX4) arising from iron-dependent ROS accumulation contributes to the initiation of ferroptosis in cancer cells.¹⁰ Recent studies revealed that erastin, a ferroptosis inducer, could remarkably increase the cytotoxic effects of cisplatin to effectively eliminate tumor cells.¹¹ Moreover, it was reported that GPX4-knockdown cells, which are sensitive to ferroptosis, had a higher survival rate than GPX4-positive cells in a diffuse large B-cell lymphoma in vitro model.¹² Additionally, siramesine and lapatinib showed potential therapeutic value in BC due to their ability to cause ferroptosis by promoting ROS accretion.^{13,14} Collectively, these findings strongly indicated that intervention targeting ferroptosis might be a potential breakthrough in the treatment of BC.

Levistilide A (LA) is an active compound extracted from Chuanxiong Rhizoma that is widely used for cancer treatment in traditional oriental medicine. Previous research showed that LA could suppress liver fibrosis by lessening sinusoid capillarization.¹⁵ In addition, LA could improve the proliferation of hepatic stellate cells by regulating the cell cycle and apoptosis.¹⁶ More importantly, it was found that LA was able to facilitate the apoptosis of colon cancer cells through a ROS accumulation-induced endoplasmic reticulum stress pathway.¹⁷ Taken together, these data indicate that LA administration may prevent the development of tumors by regulating the critical cellular processes of ferroptosis. However, at present, the specific role of LA in BC remains elusive. Therefore, in this study, we sought to explore the underlying mechanisms of LA on ferroptosis in BC.

Materials and Methods

Chemicals and Antibodies

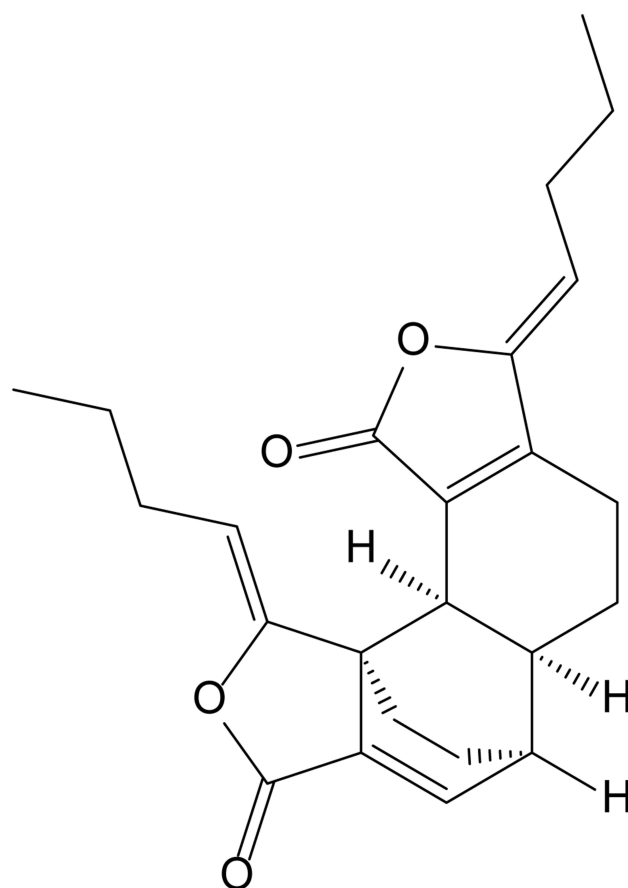
Levistilide A (purity>98%) was purchased from Chengdu Push Biological Polytron Technologies, Inc. (Chengdu, China). Its specific molecular structure was shown in Figure 1. 3-(4,5-Dimethylthiazol-2-yl)-2,5-diphenyltetrazolium bromide (MTT) was purchased from Sigma Chemical (St. Louis, MO, USA). The lactate dehydrogenase (LDH) Cytotoxicity Assay Kit (C0017), Calcein-AM (C2012), Dihydroethidium (DHE, S0063), Mitochondrial membrane potential detection kit (JC-1 method, C2006) were purchased from Beyotime Biotechnology Co., Ltd. (Shanghai, China). Liproxstatin-1 (HY-12726), ferrostatin-1 (HY-100579) and ML385 (HY-100523) were purchased from Med Chem Express (MCE, New Jersey, USA). The primary antibodies, including rabbit monoclonal anti-GPX4 (BM5231), rabbit polyclonal erythroid-2-related factor 2 (Nrf2, PB9290), and rabbit monoclonal anti-solute carrier family 7 membrane 11 (SLC7A11, BM5318), were obtained from BOSTER Biological Technology Co., Ltd. Rabbit monoclonal heme oxygenase 1 (HO-1, ab68477) was obtained from Abcam, Inc. The secondary antibody Alexa Fluor 594 anti-Rabbit IgG (8889S, CST) was obtained from Cell Signaling Technology, Inc.

Cell Culture

The human MDA-MB-231 and MCF-7 BC cell lines (source: ATCC) were provided by Guangzhou Jennio Biotech Co., Ltd. (Guangzhou, China). Cells were cultured at 37 °C in an atmosphere of 5% CO₂ in Dulbecco's modified Eagle medium (DMEM; Gibco, United States) supplemented with 10% fetal bovine serum (FBS; Gibco, United States) and 1% penicillin/streptomycin (Cat# 15140163, Thermo Fisher Scientific).

Cell Viability Assay

The cellular viability was determined by using the MTT assay. MDA-MB-231 and MCF-7 cells were seeded in 96-well plates at a density of 5×10^3 cells per well. After treatment with different concentrations of LA (0, 0.625, 1.25, 2.5, 5, 10, 20, 40, 80 μ M) for 24 h or 48 h, a total of 10 μ L of MTT solution was added to each well and incubated in the dark at 37 °C for 4 h. Next, the supernatant was discarded, and 150 μ L of dimethyl sulfoxide (#D806645, Sigma, USA) was added to each well. Then, the plates were shaken on an oscillator at a low speed for 10 min. Finally, the absorbance was measured at 570 nm by a microplate reader (Countster, United States), and the cell viability of MDA-MB-231 and MCF-7 cells was presented as a percentage of the control.



Levistilide A

CAS:88182-33-6

Figure 1 The molecular structure and Chemical Abstracts Service (CAS) number of levistilide A (LA).

LDH Assay

LDH leakage from primary GCs into the culture medium was assessed using an LDH Cytotoxicity Assay Kit (C0016, Beyotime, China). MDA-MB-231 and MCF-7 cells (1×10^5 cells/well) were seeded in 96-well plates at a density of 1×10^4 cells per well. After treatment with different concentrations of LA (0, 0.625, 1.25, 2.5, 5, 10, 20, 40, 80 μM) for 24 or 48 h, the supernatant was discarded, and 150 μL of LDH solution was added to each well. After 1 h of incubation, the supernatant was collected. Finally, the OD value was measured at 490 nm by a microplate reader (Countster, United States), and the amounts of LDH released from MDA-MB-231 and MCF-7 cells are presented as a percentage of the control.

Calcein-AM Assay

A calcein-AM assay was carried out to evaluate the effect of LA administration on apoptosis in both MDA-MB-231 and MCF-7 cells. Briefly, MDA-MB-231 and MCF-7 cells were seeded in 96-well plates (5×10^3 cells per well). After treatment with LA (0, 10, 20 and 40 μM) for 24 h, the cells were incubated with 2 μM calcein-AM (C2012, Beyotime, China) for 1 h at 37 $^\circ\text{C}$ in the dark. Then, the cells were washed three times with PBS, and the medium was replaced with fresh medium. Afterwards, the samples were observed and imaged by a fluorescence microscope (DMI8, Leica, Germany).

DHE Fluorescence Staining

Intracellular ROS levels were detected by using fluorescent DHE staining. DHE can freely enter living cells and can be oxidized to fluorescent ethidium oxide by intracellular ROS. MDA-MB-231 and MCF-7 cells were seeded in 96-well plates at a density of 5×10^3 cells per well. After treatment with LA (0, 10, 20 and 40 μM) for 24 h, the cells were fixed with 4% PFA and incubated with 5 μM DHE (S0063, Beyotime, China) for 30 min at 37 °C in the dark. Afterwards, the cells were rinsed with PBS three times to remove extra DHE. Finally, they were observed and photographed by a fluorescence microscope (DMI8, Leica, Germany). The fluorescence intensity was calculated by a Cytation imaging reader (BioTek, USA), and the quantitative data are expressed as fluorescence intensity relative to the control group.

Detection of Mitochondrial Membrane Potential (MMP)

MMP ($\Delta\psi\text{m}$) was measured by a JC-1 detection kit (C2006, Beyotime, China). MDA-MB-231 cells were seeded in 96-well plates at a density of 5×10^3 cells per well. After treatment with LA (0, 10, 20 and 40 μM) for 24 h, the cells were incubated with JC-1 staining solution for 30 min at 37 °C. JC-1 monomers and aggregates were observed with the GFP channel and Cy3 channel of a fluorescence microscope, respectively (DMI8, Leica, Germany). The fluorescence intensity was analyzed by ImageJ, and the ratio of green/red fluorescence was calculated in each group.

Transmission Electron Microscopy (TEM)

Transmission electron microscopy was used to observe the mitochondrial ultrastructure. MDA-MB231 and MCF-7 cells were seeded at a density of 1×10^6 cells/well into 100-mm plates. After treatment with LA (40 μM) for 24 h, the cells were fixed with 2.5% glutaraldehyde for 4 h and postfixed with 1% osmium tetroxide for 1 h. Then, the samples were dehydrated by a graded series of ethanol concentrations (50%, 70%, 80%, 90%, and 100%) for 15 min per concentration and embedded in Embed 812 resin. Finally, the samples were observed using a JEM2000EX transmission electron microscope (TEM, Tokyo, Japan).

Immunofluorescence Staining

Immunofluorescence staining was performed as described previously with a few modifications. MDA-MB231 and MCF-7 cells were seeded into 96-well plates at a density of 5×10^3 cells/well. Cells were fixed with 4% paraformaldehyde after 24 hours of drug treatment. Then, they were permeabilized in 0.2% Triton X-100 and blocked with 10% goat serum for 30 min. After incubated with primary antibodies, including rabbit anti-GPX4 (1:200, BM5231, BOSTER), rabbit anti-Nrf2 (1:200, PB9290, BOSTER) and rabbit anti-HO-1 (1:200, ab68477, Abcam) at 4 °C for 48 h, the samples were stained with Alexa Fluor 594-conjugated anti-rabbit IgG (8889S, CST) secondary antibody at room temperature for 2 h in the dark. After they were washed three times, the samples were stained with DAPI for 5 min. Finally, they were imaged with a fluorescence microscope (DMI8, Leica, Germany).

Real-Time Polymerase Chain Reaction (RT-PCR)

MDA-MB231 and MCF-7 cells were seeded into 6-well plates at a density of 1×10^6 cells/well. After MDA-MB-231 cells were treated with LA (0, 20 and 40 μM), total RNA was extracted by using TRIzol reagent (TaKaRa, Dalian, China). Then, the RNA concentration was detected by a NanoDrop 2000 (Thermo Fisher Scientific, USA). One microgram of total RNA was used for reverse transcription with a TAKARA PrimeScript RT reagent kit (TaKaRa, Japan). Then, real-time PCR was performed with SYBR premix Ex Taq (Takara, Japan) and conducted by using a real-time PCR system. The primer sequences are listed in Table 1. The real-time PCR data were analyzed using the value $2^{-\Delta\Delta\text{Ct}}$, and GAPDH was utilized as the housekeeping gene.

Statistical Analysis

All results are expressed as the mean \pm standard deviation (SD) from at least three independent experiments. GraphPad Prism 8.0 was utilized to carry out all statistical analyses. Statistical significance was assessed using one-way analysis of

Table 1 Primer Sequences for qPCR Detection

Gene Name	Primer Sequence (5'-3')	
	Forward	Reverse
SLCA11	TCTCAAAGGAGGTTACCTGC	AGACTCCCCTCAGTAAAGTGAC
SLC3A2	TGAATGAGTTAGAGCCCGAGA	GTCTTCCGCCACCTTGATCTT
TFRC	ACCATTGTCATATACCCGTTCA	CAATAGCCCAAGTAGCCAATCAT
SLC11A2	TGGAGATCATGGGGAGTCTG	AAGAAAACCTGGTCCGGTGAA
GCLM	CATTACAGCCTTACTGGGAGG	ATGCAGTCAAATCTGGTGGCA
GCLC	GGAGACCAGAGTATGGGAGTT	CCGGCGTTTTTCGCATGTTG
GSS	GGGAGCCTCTTGCAAGATAAA	GAATGGGGCATAGCTCACCAC
NCOA4	GAGGTGTAGTGATGCACGGAG	GACGGCTTATGCAACTGTGAA
GPX4	GAGGCAAGACCGAAGTAAACTAC	CCGAAGTGGTTACACGGGAA
NFE2L2	TCAGCGACGGAAAGAGTATGA	CCACTGGTTTCTGACTGGATGT
Hmox1	AAGACTGCGTTCCTGCTCAAC	AAAGCCCTACAGCAACTGTGC
GAPDH	GGAGCGAGATCCCTCCAAAAT	GGCTGTTGTCATACTTCTCATGG

variance (ANOVA) with a least significant difference (LSD) test for the comparison of multiple groups, and $P < 0.05$ was considered to indicate a significant difference.

Results

LA Cytotoxic Effect on BC Cells

To verify the cytotoxic effect of LA administration on BC cells, we detected the viability of MDA-MB-231 and MCF-7 cells treated with LA by the MTT assay. The results showed that LA treatment had an obvious cytotoxic effect on BC cells in a dose-dependent manner (Figure 2A and B). Moreover, the results of the LDH assay showed that LA treatment had significant cytotoxicity effects on BC cells in a dose-dependent manner (Figure 2C and D). The calcein-AM staining assay results also revealed that LA treatment remarkably promoted BC cell damage and death (Figure 2E).

LA Induced a Depolarization of MMP in BC Cells

To investigate the effect of LA on lipid peroxidation in BC cells, we evaluated the level of ROS using DHE staining analysis. As shown in Figure 3A and B, the results showed that LA administration dramatically increased the level of ROS in both MDA-MB-231 and MCF-7 cells in comparison with the control, suggesting that LA could promote ROS accumulation in BC cells. To assess the effect of LA treatment on the MMP of BC cells, we performed JC-1 staining to measure the MMP. The results showed that LA treatment markedly suppressed the MMP of BC cells relative to that of the control, which indicated that LA treatment could induce a depolarization of MMP in BC cells (Figure 3C and D). Furthermore, the smaller mitochondria with condensed mitochondrial membrane densities, the disappearance of mites, and the rupture of mitochondria are the main features of ferroptosis.¹⁸ In this study, shrunken mitochondria with cristae broken or that were disappeared were observed in both MDA-MB-231 and MCF-7 cells treated with LA, which indicated that LA treatment obviously enhanced the morphological damage in the mitochondria (Figure 3E).

LA Promoted Ferroptosis in BC Cells

To determine whether LA exerted an antitumor effect by promoting ferroptosis in BC cells, we detected the expression of key molecules in the ferroptosis pathway. GPX4 is an antioxidant enzyme that can prevent lipid peroxide accumulation against ferroptosis using glutathione (GSH) as a cofactor.^{18,19} Notably, GSH cannot function as a reducing agent within the local peroxidase reaction cycle and thus causes an accumulation of lipid ROS and the induction of ferroptosis without adequate levels of GPX4.²⁰ Recent studies have pointed out that the loss of GPX4 activity leads to the formulation of high ROS and subsequent ferroptosis.²¹ In this work, the results showed that LA treatment remarkably inhibited the expression of GPX4 in both MDA-MB-231 (Figure 4A and C) and MCF-7 cells (Figure 4B and D) in a dose-dependent

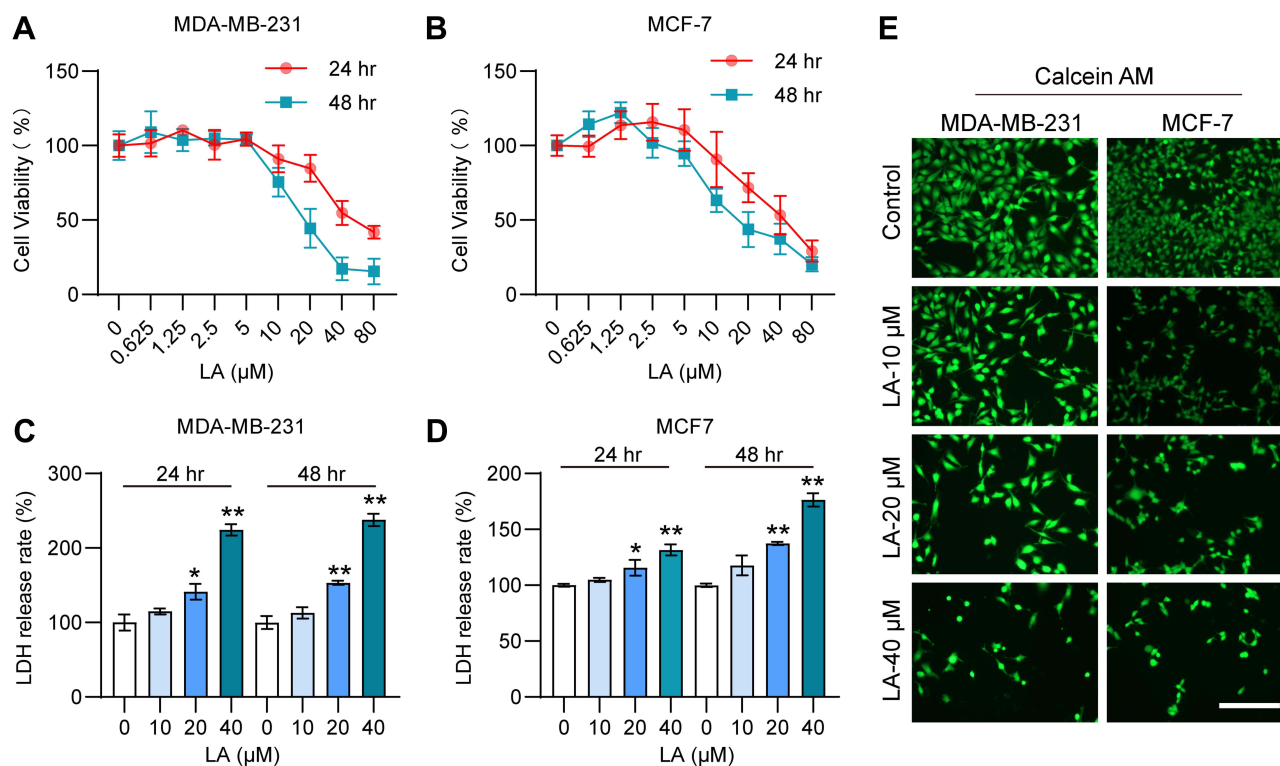


Figure 2 LA had a cytotoxic effect on MDA-MB-231 and MCF-7 cells. MDA-MB-231 and MCF-7 cells were cultured in 96-well plates and treated with the corresponding concentrations of LA for 24 or 48 h. The effect of LA on the viability of MDA-MB-231 and MCF-7 cells was tested by MTT assay, LDH assay and Calcein-AM assay. **(A)** The viability of MDA-MB-231 cells was determined in different groups. **(B)** The viability of MCF-7 cells was determined in different groups. **(C)** The LDH release rate of MDA-MB-231 cells was determined in different groups. **(D)** The LDH release rate of MCF-7 cells was determined in different groups. **(E)** The effect of LA on the viability of MDA-MB-231 and MCF-7 cells was tested by a calcein-AM assay. Bar=200 μm. The experiments were repeated at least three times with 3 replicates, and data are expressed as the mean ± SD. **P* <0.05, ***P* <0.01 compared with the control group.

manner. System Xc⁻ is an indispensable player with a heterodimeric cystine/glutamate antiporter composed of SLC7A11 and SLC3A2. It can exchange intracellular glutamate for extracellular cystine, thereby supporting intracellular GSH synthesis.²² Interestingly, LA treatment led to a compensatory increase in the mRNA expression of SLC7A11 and SLC3A2 in MDA-MB-231 cells. Glutamate-cysteine ligase (GCL), which consists of catalytic (GCLC) and modifier (GCLM) subunits, and glutathione synthetase (GSS) are two key rate-limiting enzymes of GSH synthesis.²³ In this work, LA administration also resulted in a compensatory upregulation of GCLC, GCLM and GSS mRNA expression in MDA-MB-231 cells. Moreover, a compensatory increase in intracellular iron transporters transferrin receptor (TFRC) and solute carrier family 11 membrane 2 (SLC11A2) mRNA expression was observed in MDA-MB-231 cells treated with LA. These findings strongly suggested that LA treatment mainly induced ferroptosis in BC cells by promoting ROS accumulation by inhibiting GPX4 expression. Nuclear receptor coactivator 4 (NCOA4) is a choosy cargo receptor for ferritinophagy. Recent studies have shown that NCOA4 overexpression reinforces ferritin degradation and then drives ferroptosis.²⁴ In this work, the mRNA expression of NCOA4 was obviously increased in MDA-MB-231 cells treated with LA (Figure 4E).

LA Upregulated the Nrf2/HO-1 Signaling Pathway in BC Cells

Previous studies reported that the overexpression of HO-1 could augment ferroptosis in tumor cells.²⁵ Therefore, in this work, to explore whether LA administration promoted ferroptosis in BC cells by upregulating HO-1, the expression of HO-1 and its upstream molecule Nrf2 in both MDA-MB-231 (Figure 5A and B) and MCF-7 cells (Figure 5A and C) was detected. The results showed that LA treatment obviously increased the protein levels of Nrf2 and HO-1 in both MDA-MB-231 and MCF-7 cells. Moreover, LA administration significantly enhanced the mRNA expression levels of Nrf2 and HO-1 in MDA-MB-231 cells (Figure 5D).

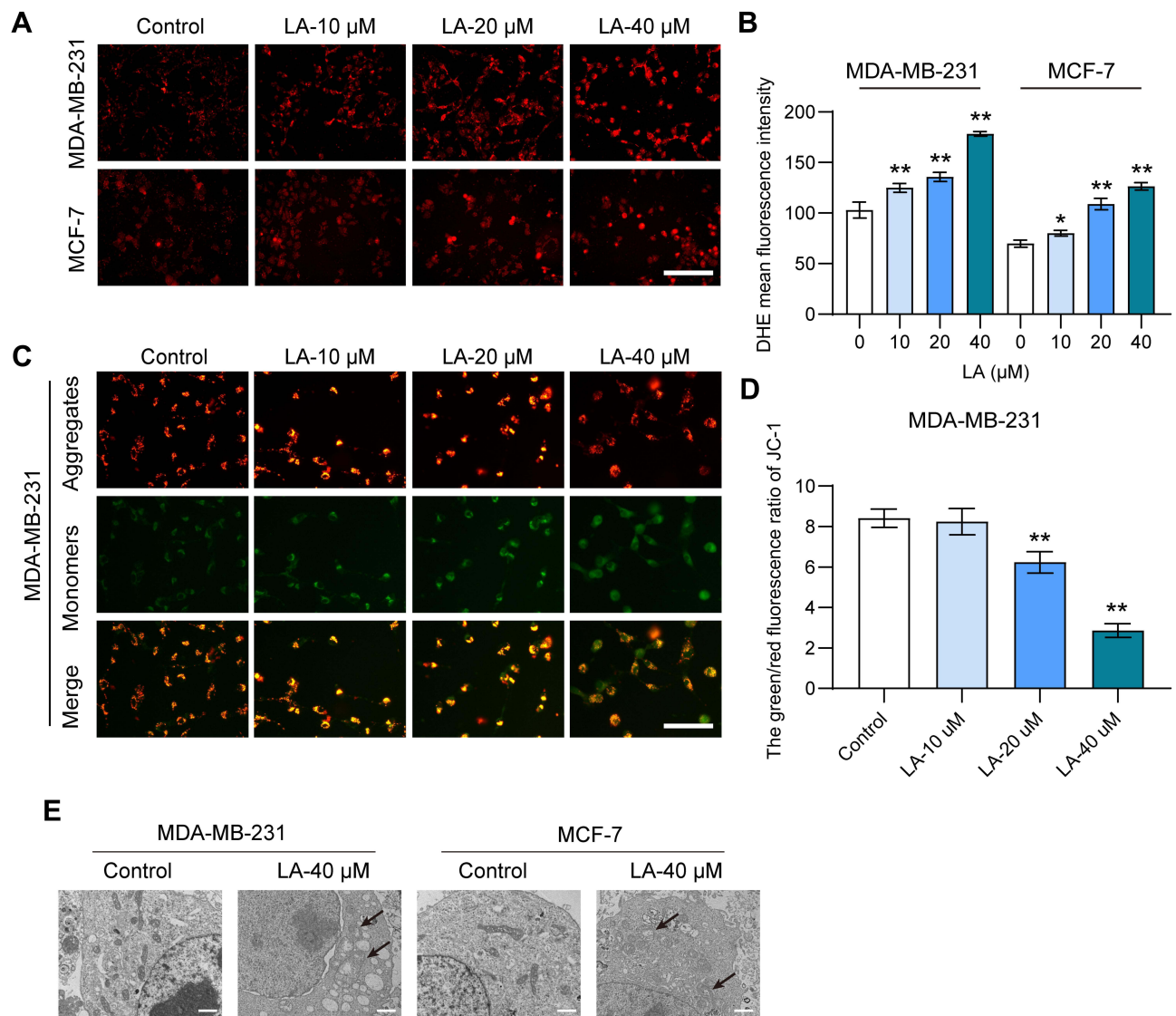


Figure 3 LA suppressed the mitochondrial function of MDA-MB-231 and MCF-7 cells. MDA-MB-231 and MCF-7 cells were cultured in 96-well plates and treated with the corresponding concentrations of LA for 24 h. The effect of LA on the mitochondrial function of MDA-MB-231 and MCF-7 cells was tested by a DHE staining assay, JC-1 staining assay and TEM assay. **(A)** The fluorescence intensity of DHE represents the ROS concentration in different groups. Bar=200 μm. **(B)** Statistical analysis of DHE fluorescence intensity in MDA-MB-231 and MCF-7 cells treated with LA. **(C)** The fluorescence intensity of JC-1 in MDA-MB-231 cells between different groups. Bar=400 μm. **(D)** Statistical analysis of JC-1 fluorescence intensity in MDA-MB-231 cells treated with LA. **(E)** TEM images of mitochondrial morphology were obtained and compared between different groups. Black arrows indicate damaged mitochondria, Bar=2 μm. The experiments were repeated at least three times with 3 replicates, and data are expressed as the mean ± SD. * $P < 0.05$, ** $P < 0.01$ compared with the control group.

Ferroptosis and Nrf2 Inhibitors Diminished the Cytotoxic Effect of LA in BC Cells

To further investigate whether LA treatment promoted BC cell death by facilitating ferroptosis via the Nrf2/HO-1 signaling pathway, BC cells treated with LA were incubated with the ferroptosis inhibitor Liproxstain-1 and the Nrf2 inhibitor ML385. The results showed that the cytotoxic effect of LA on MDA-MB-231 cells was significantly diminished by the above inhibitors (Figure 6A). These findings further revealed that LA facilitated BC cell death by inducing ferroptosis via the Nrf2/HO-1 pathway (Figure 6B–G).

Discussion

LA, as a phthalide dimer isolated from Chuanxiong Rhizoma, has been reported to have effective anti-fibrotic and anticancer effects in several diseases. Therefore, in this study, the effect of LA treatment on BC cells was evaluated. The results showed that

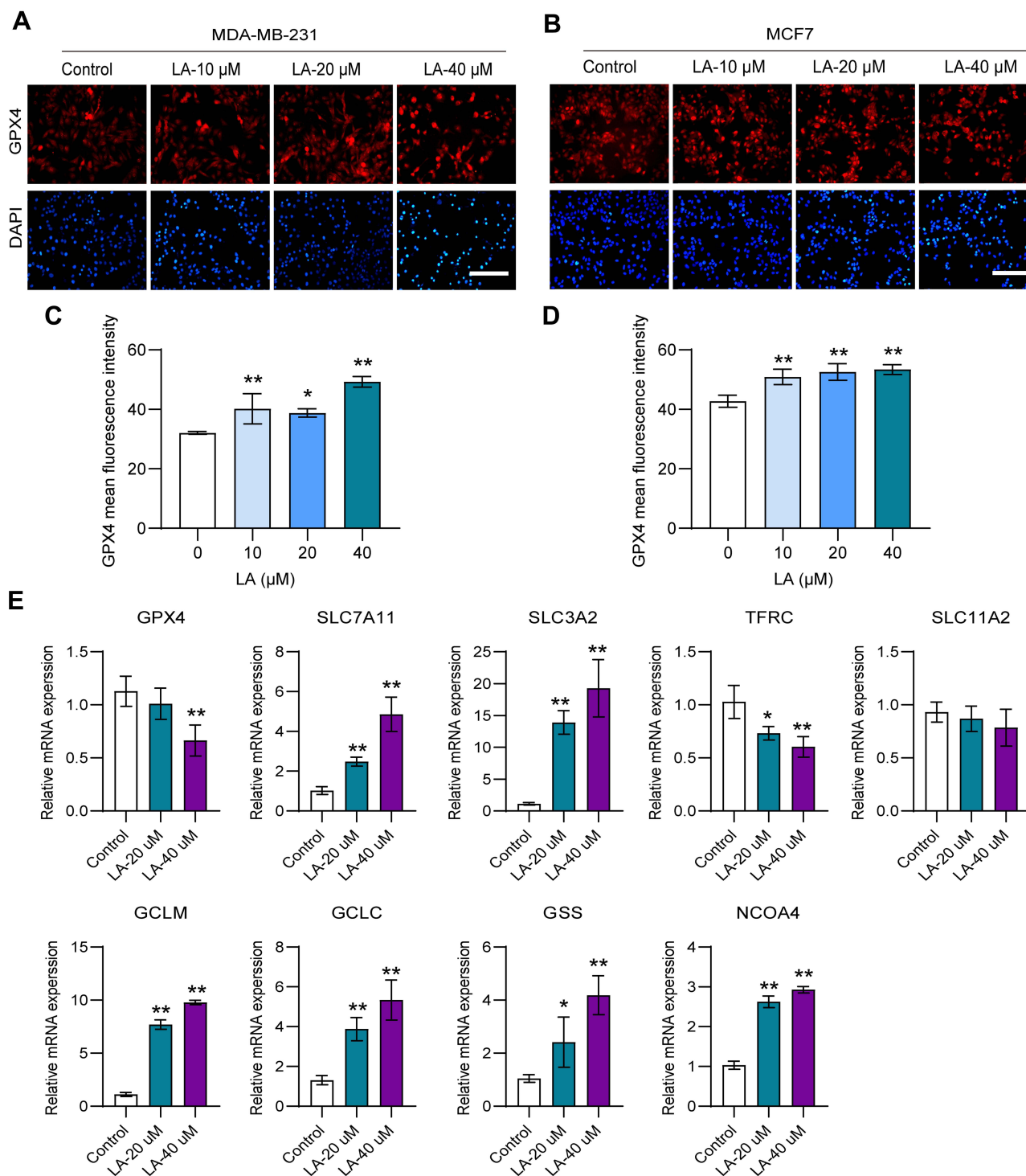


Figure 4 LA promoted ferroptosis in BC cells. MDA-MB-231 and MCF-7 cells were cultured in 96-well plates and treated with the corresponding concentrations of LA for 24 h. The effect of LA on the expression of GPX4 in MDA-MB-231 and MCF-7 cells was tested by immunofluorescence staining, and the expression of ferroptosis-related mRNA in MDA-MB-231 cells was tested using RT-qPCR. (A) GPX4 expression was analyzed using immunofluorescence staining in MDA-MB-231 cells. Bar=200 μm. (B) GPX4 expression was analyzed using immunofluorescence staining in MCF-7 cells. (C) Statistical analysis of GPX4 fluorescence intensity in MDA-MB-231 cells treated with LA. (D) Statistical analysis of GPX4 fluorescence intensity in MCF-7 cells treated with LA. (E) The expression of ferroptosis-related mRNAs in MDA-MB-231 cells was analyzed using RT-qPCR. The experiments were repeated at least three times with 3 replicates, and data are expressed as the mean ± SD. **P* < 0.05, ***P* < 0.01 compared with the control group.

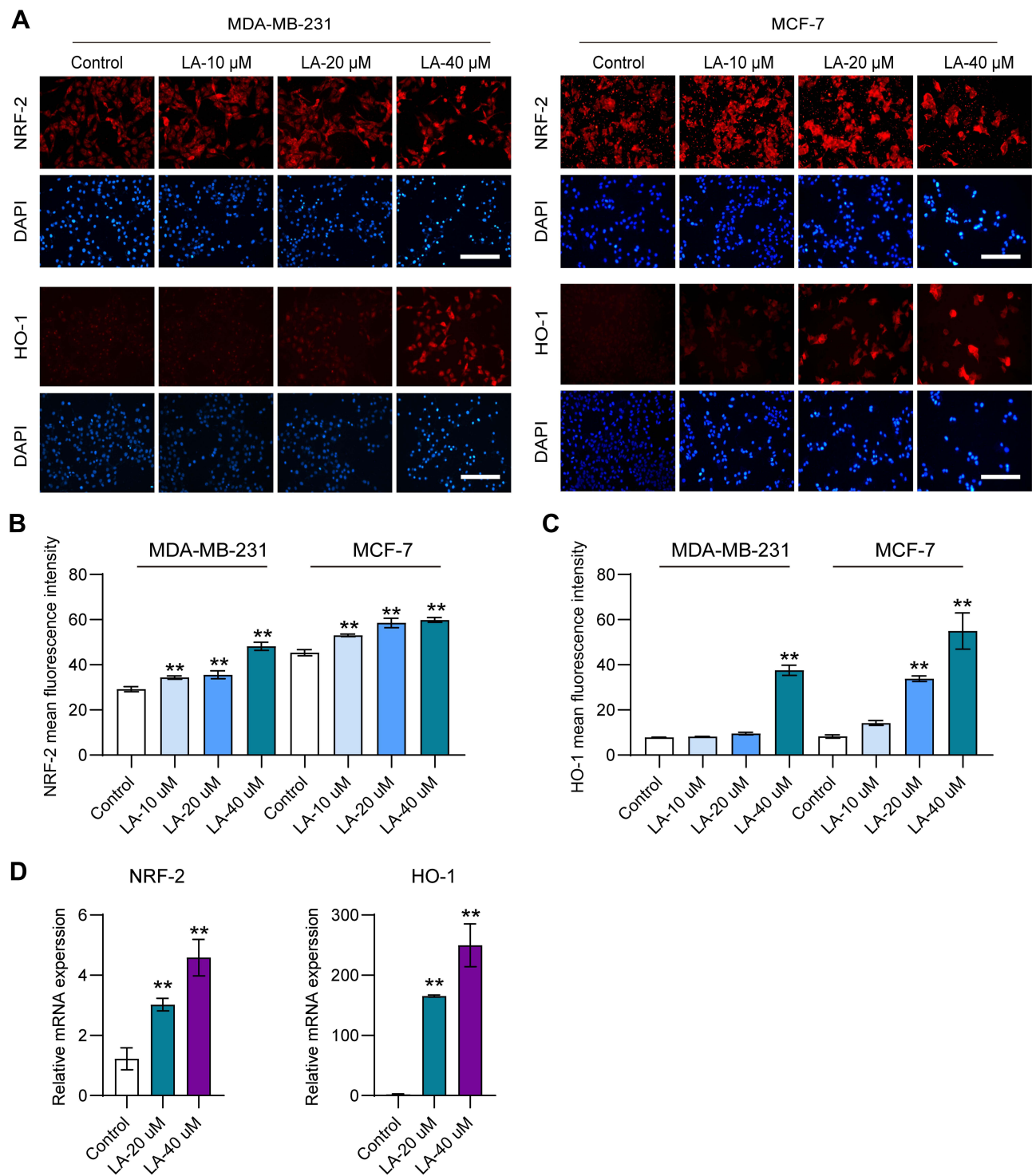


Figure 5 LA upregulated the Nrf2/HO-1 signaling pathway in BC cells. MDA-MB-231 and MCF-7 cells were cultured in 96-well plates and treated with the corresponding concentrations of LA for 24 h. The effect of LA on the expression of Nrf2 and HO-1 in MDA-MB-231 and MCF-7 cells was tested by immunofluorescence staining and RT-qPCR. **(A)** The expression of Nrf2 and HO-1 in MDA-MB-231 and MCF-7 cells was analyzed using immunofluorescence staining. Bar=200 μ m. **(B)** Statistical analysis of Nrf2 fluorescence intensity in MDA-MB-231 and MCF-7 cells treated with LA. **(C)** Statistical analysis of HO-1 fluorescence intensity in MDA-MB-231 and MCF-7 cells treated with LA. **(D)** The relative mRNA expression of Nrf2 and HO-1 in MDA-MB-231 cells was analyzed using RT-qPCR. The experiments were repeated at least three times with 3 replicates, and data are expressed as the mean \pm SD. ** P < 0.01 compared with the control group.

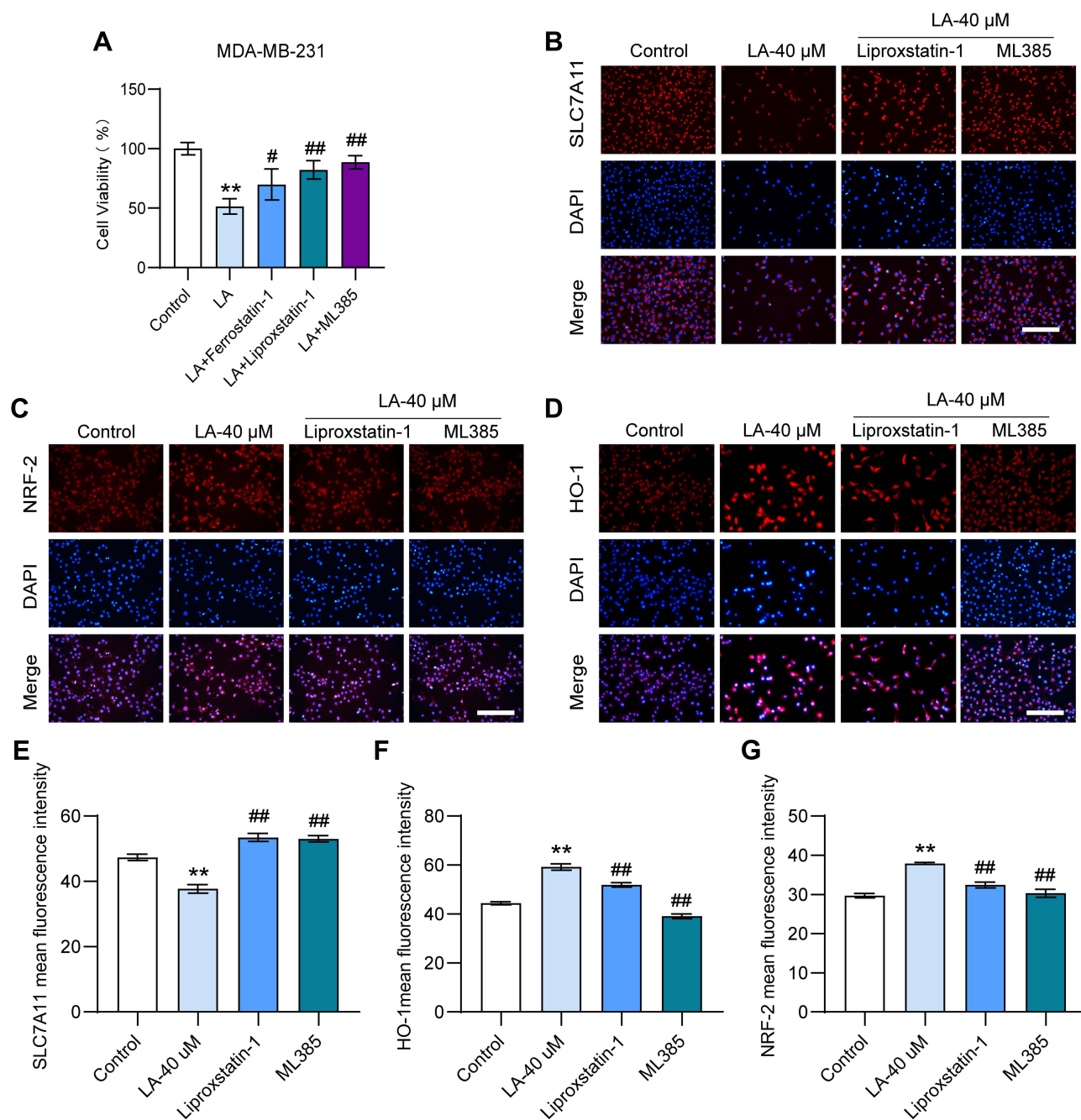


Figure 6 Ferroptosis or Nrf2 inhibitors diminished the cytotoxic effect of LA in BC cells. MDA-MB-231 cells were cultured in 96-well plates. Ferrostatin-1 (2.5 μM) or lipoxstatin-1 (2 μM) were used as ferroptosis inhibitors, and ML385 (10 μM) was selected as Nrf2 inhibitors. All inhibitors were incubated with LA (40 μM) for 24 hours. The viability of MDA-MB-231 cells was tested by MTT assay, and the expressions of SLC7A11, Nrf2 and HO-1 were detected using immunofluorescence staining. (A) The viability of MDA-MB-231 cells was determined in different groups. (B-D) The expressions of SLC7A11, Nrf2 and HO-1 in MDA-MB-231 cells. The experiments were repeated at least three times with 3 replicates, and data are expressed as the mean ± SD. ***P* < 0.01 compared with the control group, #*P* < 0.05, ##*P* < 0.01 compared with the LA-treated group.

LA administration exhibited significant cytotoxicity against MDA-MB-231 and MCF-7-cell lines in a dose-dependent manner. These beneficial properties impel us to further determine the underlying mechanism of LA on BC.

Iron is an essential element involved in a wide variety of biological activities and plays a vital role in regulating the tumor microenvironment and metastasis. It has been reported that iron overload could exacerbate ROS-mediated oxidative stress through the Fenton reaction in tumor cells.²⁶ Mitochondria represent both the primary source of ROS and the main target of ROS damage.²⁷ Importantly, an excessive level of ROS is a marker of lethal lipid

peroxidation, which can damage the DNA and proteins of tumor cells and lead to cell death. Recent studies have pointed out that the augmentation of ROS might be the key tumor suppression mechanism to prevent the outgrowth of tumor cells.²⁸ Several chemotherapeutic drugs, such as cisplatin and 5-fluorouracil, have been reported to have anticancer effects by promoting apoptosis induced by ROS overproduction.²⁹ Previous research found that LA treatment had anticancer effects in colon cancer cells by increasing intracellular ROS levels.¹⁷ In this study, it was found that LA administration dramatically enhanced ROS accumulation and mitochondrial morphology and function impairment in BC cells. These findings strongly indicated that LA treatment could cause ROS-induced lethal oxidative damage to tumor cells.

Ferroptosis is an iron dependent, nonapoptotic cell death modality characterized by aberrant intracellular ROS accumulation. ROS overproduction could lead to lipid peroxidation and destroy the normal structure and function of mitochondria, eventually causing ferroptosis.³⁰ A great deal of evidence suggests that ferroptosis plays an indispensable role in the process of tumor inhibition.^{31,32} Recent studies have pointed out that a subset of tumor cells are highly sensitive to ferroptosis due to their dependence on the oxidative stress environment.^{32,33} Importantly, several ferroptosis inducers, such as erastin and RSL3, have potent therapeutic effects on cancer treatment.^{34,35} GPX4 is a key regulator of ferroptosis in cancer cells that protects cells from oxidative stress damage, and the inhibition of GPX4 activity indeed induces ROS accumulation and subsequent ferroptosis.^{36,37} In this work, it was found that LA treatment significantly inhibited the expression of GPX4 in BC cells. Furthermore, the depletion of GPX4 led to compensatory mRNA overexpression of GSH synthesis rate-limiting enzymes, such as GCLM, GCLC and GSS, in LA-treated MDA-MB-231 cells. Interestingly, LA treatment also caused a compensatory increase in SLC7A11 and SLC3A2 mRNA expression. Recent studies pointed out that high SLC7A11 expression could lead to metabolic vulnerability in cancer cells, resulting in a high dependence on glutamine for their survival and proliferation.³⁸ Iron combines with transferrin and then enters the cells via TFRC and the divalent metal ion transporter SLC11A2.³⁹ In this study, GPX4 depletion produced a compensatory increase in TFRC and SLC11A2 mRNA expression in BC cells treated with LA. Moreover, it has been reported that NCOA4 overexpression could induce ferritin degradation and then induce ferroptosis.⁴⁰ In this work, it was found that LA administration significantly enhanced NCOA4 mRNA expression in MDA-MB-231 cells in a dose-dependent manner. These findings suggested that GPX4 depletion-induced ferroptosis was the main mechanism by which LA exerted anticancer effects in BC cells.

HO-1 degrades hemoglobin into iron, carbon monoxide and biliverdin, which play vital roles in cancer progression as dual regulators.⁴¹ On the one hand, HO-1 was reported to protect tumor cells against oxidative stress, thus preventing them from undergoing apoptosis. On the other hand, recent studies revealed that the increased expression of HO-1 can augment ferroptosis by enhancing iron production and can eventually lead to ROS accumulation in tumor cells.^{42,43} These contradictory effects might depend on the degree of intracellular iron levels and subsequent lipid oxidative damage in response to cues. In this study, it was found that LA administration could significantly enhance ferroptosis by upregulating the expression of HO-1 and its upstream molecule Nrf2. These data strongly indicated that LA promoted the overexpression of the Nrf2/HO-1 axis and further enhanced the excessive intracellular accumulation of iron and ROS, eventually leading to ferroptosis in BC cells.

To further investigate whether LA treatment suppresses ferroptosis via the Nrf2/HO-1 signaling pathway, MDA-MB-231 cells were incubated with the ferroptosis inhibitor Liproxstain-1 and the Nrf2 inhibitor ML385. The results showed that the cytotoxic effect of LA administration on BC cells was significantly diminished by the above inhibitors. These findings further verified that LA treatment could facilitate BC cell death by inducing ferroptosis via the Nrf2/HO-1 axis.

Conclusion

In this study, it was found that LA administration could significantly reduce cell viability and induce mitochondrial structure and function damage in BC cells in a dose-dependent manner. Furthermore, it was verified that LA treatment effectively promoted ROS-induced ferroptosis by activating the Nrf2/HO-1 signaling pathway in BC cells (Figure 7). Taken together, these findings suggest that LA is a potential therapeutic drug in the treatment of BC.

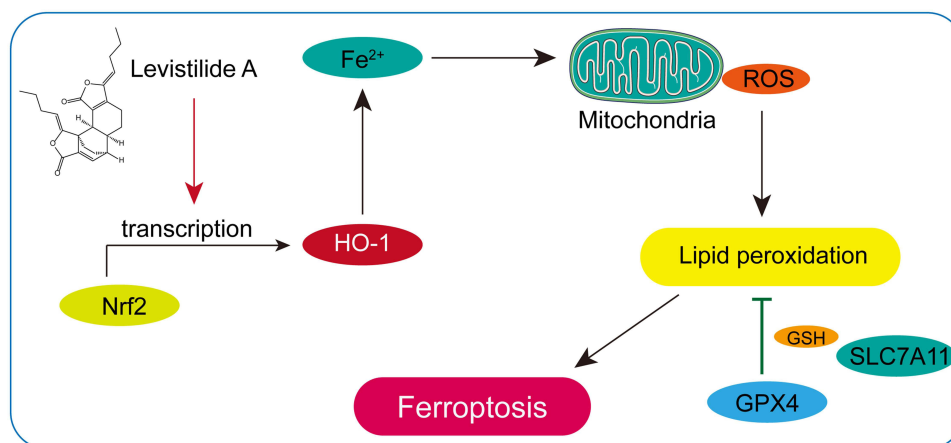


Figure 7 Schematic illustration of LA-induced ferroptosis in BC cells through activation of the Nrf2/HO-1 pathway.

Funding

This work was supported by the National Natural Science Foundation of China (No. 81774261), Guangdong Province Science and Technology Plan International Cooperation Project (No. 2020A0505100052), Natural Science Foundation of Guangdong Province (No. 2022A1515011260), Guangzhou Science and Technology Plan Project (No. 202002020033), and Guangzhou Science and Technology Plan Project (202102010178).

Disclosure

The authors declare no conflicts of interest for this work.

References

- Jatoi I, Kemp Z. Surgery for breast cancer prevention. *JAMA*. 2021;325(17):1804. doi:10.1001/jama.2021.1647
- Lu YS, Yeo W, Yap YS, et al. An overview of the treatment efficacy and side effect profile of pharmacological therapies in asian patients with breast cancer. *Target Oncol*. 2021;16(6):701–741. doi:10.1007/s11523-021-00838-x
- Reeves C. San antonio breast cancer symposium 2021. *Lancet Oncol*. 2022;23(1):e18. doi:10.1016/S1470-2045(21)00727-0
- Chikatani K, Chika N, Suzuki O, et al. Clinically applicable cases of anti-programmed cell death protein 1 immunotherapy for colorectal cancer patients. *Surg Today*. 2020;50(12):1694–1698. doi:10.1007/s00595-020-01998-5
- Hadian K, Stockwell BR. SnapShot: ferroptosis. *Cell*. 2020;181(5):1188–1188.e1. doi:10.1016/j.cell.2020.04.039
- Xu H, Ye D, Ren M, Zhang H, Bi F. Ferroptosis in the tumor microenvironment: perspectives for immunotherapy. *Trends Mol Med*. 2021;27(9):856–867. doi:10.1016/j.molmed.2021.06.014
- Stockwell BR, Jiang X, Physiologica A. Function for ferroptosis in tumor suppression by the immune system. *Cell Metab*. 2019;30(1):14–15. doi:10.1016/j.cmet.2019.06.012
- Yuan LQ, Wang C, Lu DF, Zhao XD, Tan LH, Chen X. Induction of apoptosis and ferroptosis by a tumor suppressing magnetic field through ROS-mediated DNA damage. *Aging*. 2020;12(4):3662–3681. doi:10.18632/aging.102836
- Yao X, Li W, Fang D, et al. Emerging roles of energy metabolism in ferroptosis regulation of tumor cells. *Adv Sci*. 2021;8(22):e2100997. doi:10.1002/advs.202100997
- Zou Y, Palte MJ, Deik AA, et al. A GPX4-dependent cancer cell state underlies the clear-cell morphology and confers sensitivity to ferroptosis. *Nat Commun*. 2019;10(1):1617. doi:10.1038/s41467-019-09277-9
- Li Y, Yan H, Xu X, Liu H, Wu C, Zhao L. Erastin/sorafenib induces cisplatin-resistant non-small cell lung cancer cell ferroptosis through inhibition of the Nrf2/xCT pathway. *Oncol Lett*. 2020;19(1):323–333. doi:10.3892/ol.2019.11066
- Weng J, Chen L, Liu H, Yang XP, Huang L. Ferroptosis markers predict the survival, immune infiltration, and ibrutinib resistance of diffuse large B cell Lymphoma. *Inflammation*. 2022;45:1146–1161. doi:10.1007/s10753-021-01609-6
- Villalpando-Rodriguez GE, Blankstein AR, Konzelman C, Gibson SB. Lysosomal destabilizing drug siramesine and the dual tyrosine kinase inhibitor lapatinib induce a synergistic ferroptosis through reduced heme oxygenase-1 (HO-1) levels. *Oxid Med Cell Longev*. 2019;2019:9561281. doi:10.1155/2019/9561281
- Jia JN, Yin XX, Li Q, et al. Neuroprotective effects of the anti-cancer drug lapatinib against epileptic seizures via suppressing glutathione peroxidase 4-dependent ferroptosis. *Front Pharmacol*. 2020;11:601572. doi:10.3389/fphar.2020.601572
- Zhao ZM, Liu HL, Sun X, et al. Levistilide A inhibits angiogenesis in liver fibrosis via vascular endothelial growth factor signaling pathway. *Exp Biol Med*. 2017;242(9):974–985. doi:10.1177/1535370217701005
- Li S, Zhao W, Zhao Z, Cheng B, Li S, Liu C. Levistilide A reverses rat hepatic fibrosis by suppressing angiotensin II-induced hepatic stellate cells activation. *Mol Med Rep*. 2020;22(3):2191–2198. doi:10.3892/mmr.2020.11326

17. Yang Y, Zhang Y, Wang L, Lee S. Levistolide A induces apoptosis via ROS-mediated ER stress pathway in colon cancer cells. *Cell Physiol Biochem*. 2017;42(3):929–938. doi:10.1159/000478647
18. Otasevic V, Vucetic M, Grigorov I, Martinovic V, Stancic A. Ferroptosis in different pathological contexts seen through the eyes of mitochondria. *Oxid Med Cell Longev*. 2021;2021:5537330. doi:10.1155/2021/5537330
19. Yan B, Ai Y, Sun Q, et al. Membrane damage during ferroptosis is caused by oxidation of phospholipids catalyzed by the oxidoreductases POR and CYB5R1. *Mol Cell*. 2021;81(2):355–369.e10. doi:10.1016/j.molcel.2020.11.024
20. Zheng J, Conrad M. The metabolic underpinnings of ferroptosis. *Cell Metab*. 2020;32(6):920–937. doi:10.1016/j.cmet.2020.10.011
21. Zhu H, Santo A, Jia Z, Robert LY. GPx4 in bacterial infection and polymicrobial sepsis: involvement of ferroptosis and pyroptosis. *React Oxyg Species*. 2019;7(21):154–160.
22. Miess H, Dankworth B, Gouw AM, et al. The glutathione redox system is essential to prevent ferroptosis caused by impaired lipid metabolism in clear cell renal cell carcinoma. *Oncogene*. 2018;37(40):5435–5450. doi:10.1038/s41388-018-0315-z
23. Chu B, Kon N, Chen D, et al. ALOX12 is required for p53-mediated tumour suppression through a distinct ferroptosis pathway. *Nat Cell Biol*. 2019;21(5):579–591. doi:10.1038/s41556-019-0305-6
24. Santana-Codina N, Gikandi A, Mancias JD. The role of NCOA4-mediated ferritinophagy in ferroptosis. *Adv Exp Med Biol*. 2021;1301:41–57.
25. Malfà GA, Tomasello B, Acquaviva R, et al. Betula etnensis raf. (Betulaceae) extract induced HO-1 expression and ferroptosis cell death in human colon cancer cells. *Int J Mol Sci*. 2019;20(11):2723. doi:10.3390/ijms20112723
26. Rodriguez R, Schreiber SL, Conrad M. Persister cancer cells: iron addiction and vulnerability to ferroptosis. *Mol Cell*. 2022;82(4):728–740. doi:10.1016/j.molcel.2021.12.001
27. Tadokoro T, Ikeda M, Ide T, et al. Mitochondria-dependent ferroptosis plays a pivotal role in doxorubicin cardiotoxicity. *JCI Insight*. 2020;5(9). doi:10.1172/jci.insight.132747
28. Wang Y, Qi H, Liu Y, et al. The double-edged roles of ROS in cancer prevention and therapy. *Theranostics*. 2021;11(10):4839–4857. doi:10.7150/thno.56747
29. Moloney JN, Cotter TG. ROS signalling in the biology of cancer. *Semin Cell Dev Biol*. 2018;80:50–64. doi:10.1016/j.semedb.2017.05.023
30. Tao W, Wang N, Ruan J, et al. Enhanced ROS-boosted phototherapy against pancreatic cancer via Nrf2-mediated stress-defense pathway suppression and ferroptosis induction. *ACS Appl Mater Interfaces*. 2022;14(5):6404–6416. doi:10.1021/acsami.1c22861
31. Lei G, Zhang Y, Hong T, et al. Ferroptosis as a mechanism to mediate p53 function in tumor radiosensitivity. *Oncogene*. 2021;40(20):3533–3547. doi:10.1038/s41388-021-01790-w
32. Mbah NE, Lyssiotis CA. Metabolic regulation of ferroptosis in the tumor microenvironment. *J Biol Chem*. 2022;298(3):101617. doi:10.1016/j.jbc.2022.101617
33. Dierge E, Debock E, Guilbaud C, et al. Peroxidation of n-3 and n-6 polyunsaturated fatty acids in the acidic tumor environment leads to ferroptosis-mediated anticancer effects. *Cell Metab*. 2021;33(8):1701–1715.e5. doi:10.1016/j.cmet.2021.05.016
34. Sui X, Zhang R, Liu S, et al. RSL3 drives ferroptosis through GPX4 inactivation and ROS production in colorectal cancer. *Front Pharmacol*. 2018;9:1371. doi:10.3389/fphar.2018.01371
35. Zhao Y, Li Y, Zhang R, Wang F, Wang T, Jiao Y. The role of erastin in ferroptosis and its prospects in cancer therapy. *Onco Targets Ther*. 2020;13:5429–5441. doi:10.2147/OTT.S254995
36. Shin D, Kim EH, Lee J, Roh JL. Nrf2 inhibition reverses resistance to GPX4 inhibitor-induced ferroptosis in head and neck cancer. *Free Radic Biol Med*. 2018;129:454–462. doi:10.1016/j.freeradbiomed.2018.10.426
37. Lee N, Carlisle AE, Peppers A, et al. xCT-driven expression of GPX4 determines sensitivity of breast cancer cells to ferroptosis inducers. *Antioxidants*. 2021;10(2):317.
38. Koppula P, Zhuang L, Gan B. Cystine transporter SLC7A11/xCT in cancer: ferroptosis, nutrient dependency, and cancer therapy. *Protein Cell*. 2021;12(8):599–620. doi:10.1007/s13238-020-00789-5
39. Guo W, Li K, Sun B, et al. Dysregulated glutamate transporter SLC1A1 propels cystine uptake via Xc(-) for glutathione synthesis in lung cancer. *Cancer Res*. 2021;81(3):552–566. doi:10.1158/0008-5472.CAN-20-0617
40. Gryzik M, Asperti M, Denardo A, Arosio P, Poli M. NCOA4-mediated ferritinophagy promotes ferroptosis induced by erastin, but not by RSL3 in HeLa cells. *Biochim Biophys Acta Mol Cell Res*. 2021;1868(2):118913. doi:10.1016/j.bbamcr.2020.118913
41. Li R, Zhang J, Zhou Y, et al. Transcriptome investigation and in vitro verification of curcumin-induced HO-1 as a feature of ferroptosis in breast cancer cells. *Oxid Med Cell Longev*. 2020;2020:3469840. doi:10.1155/2020/3469840
42. Hsieh CH, Hsieh HC, Shih FS, et al. An innovative NRF2 nano-modulator induces lung cancer ferroptosis and elicits an immunostimulatory tumor microenvironment. *Theranostics*. 2021;11(14):7072–7091. doi:10.7150/thno.57803
43. Tang Z, Ju Y, Dai X, et al. HO-1-mediated ferroptosis as a target for protection against retinal pigment epithelium degeneration. *Redox Biol*. 2021;43:101971. doi:10.1016/j.redox.2021.101971

Drug Design, Development and Therapy

Dovepress

Publish your work in this journal

Drug Design, Development and Therapy is an international, peer-reviewed open-access journal that spans the spectrum of drug design and development through to clinical applications. Clinical outcomes, patient safety, and programs for the development and effective, safe, and sustained use of medicines are a feature of the journal, which has also been accepted for indexing on PubMed Central. The manuscript management system is completely online and includes a very quick and fair peer-review system, which is all easy to use. Visit <http://www.dovepress.com/testimonials.php> to read real quotes from published authors.

Submit your manuscript here: <https://www.dovepress.com/drug-design-development-and-therapy-journal>